DOI: 10.2478/cse-2014-0002 — Catal. Sustain. Energy 2014; Volume 2: 10–20 DE GRUYTER OPEN

Research Article **Open Access**

Arapova M. V., Pavlova S. N., Rogov V. A., Krieger T. A., Ishchenko A.V., Roger A.-C.

Ni(Co)-containing catalysts based on perovskite-like ferrites for steam reforming of ethanol

Abstract: For two series of catalysts based on praseodymium ferrite, their structural and redox properties as well as performance in ethanol steam reforming have been studied. The first series was $PrFe_{1-x}Ni(Co)_xO_3$ (x=0.3-0.4) perovskites prepared by modified Pechini route, and the second one was 5%wt.Ni(Co)/$PrFeO_3$ of different dispersion prepared by impregnation of $PrFeO_3$, including samples modified by 5%wt. Mo. At temperatures above 700°C, for all catalysts, the main products were hydrogen and CO. At temperatures below 700°C, initial ethanol conversion and hydrogen yield were higher for supported catalysts as compared with ones derived from Ni(Co)-containing perovskites. While Ni-based catalysts derived from perovskite were more active as compared with Co-based samples, Co-supported $PrFeO_3$ perovskite has shown a higher initial activity as compared with Ni-supported one. The long-term tests in the realistic feed and TEM studies of spent catalysts revealed that perovskite-derived catalysts have a higher coking stability than perovskite-supported ones due to formation of highly dispersed Ni-Fe alloy particles strongly interacting with disordered perovskite–like matrix. The method of Mo supporting only slightly affects the initial activity of Ni/$PrFeO_3$–based catalysts but noticeably modifies their coking stability: 5%Mo/5%Ni/$PrFeO_3$ catalyst prepared by successive impregnation possesses the highest stability among perovskite-supported catalysts.

Keywords: Ethanol steam reforming, nickel, cobalt, praseodimium ferrite, molybdenum

***Corresponding author: Arapova M. V.:** Boreskov Institute of Catalysis, arapova@catalysis.ru
Arapova M. V., Pavlova S. N., Rogov V. A., Krieger T. A., Ishchenko A.V.: Boreskov Institute of Catalysis,
Rogov V. A.: Novosibirsk State University
Roger A.-C.: University of Strasbourg

1 Introduction

Catalytic steam reforming (SR) is now considered as the main pathway to produce hydrogen and synthesis gas from alcohols and other oxygenates derived from fast pyrolysis of biomass as a renewable feedstock [1-7]. Bio-hydrogen and bio-syngas could be used for production of liquid fuels (gasoline, diesel) and valuable chemicals production, and they are the cleanest fuels for different types of fuel cells, gas turbine, internal combustion engine as well.

The active catalysts for bio-ethanol steam reforming (ESR) are usually based on supported transition metals (Ni, Co) [8-14] or noble metals [15-19]. The major problem of ethanol SR hindering its industrial application, especially in the case of Ni-containing catalysts, is their coking leading to deactivation [8-14]. The use of perovskite-like oxides ABO_3 as catalyst precursors or supports is an attractive approach to minimize the coke deposition on catalysts. Thus, recently, in our study of methane dry reforming over $LnFe_{0.7-x}Ru_xNi_{0.3}O_{3-d}$ (Ln = La, Pr, Sm, x = 0 - 0.1) perovskites [20-21], their transformation into composites comprised of Ni-Fe-(Ru) alloy particles and LnO_x epitaxially bound with disordered Ln-Fe-O perovskite particles was demonstrated. This microstructure plays an important role in the high catalysts resistance to coking due to activation of CO_2 on the oxide sites and oxidation of CH_x fragments at alloy particles/support interface by thus formed active oxygen-containing species. The nature of Ln cation affects both the composition of Ni-Fe-(Ru) alloy and oxygen mobility/reactivity in perovskite.

In the case of oxygenates reforming, perovskites as the catalyst precursors were reported only in few works [22-27]. Thus, $LaMO_3$ (M= Ni, Co, Fe, Mn) perovskites have been studied in the authothermal reforming of ethanol [22]. Nickel-supported Ca(Sr)-substituted $La_{1-x}Ca(Sr)_xFeO_3$ perovskite oxide catalysts have shown very good stability and activity in steam reforming of ethanol [24].

Another option for improving Ni-catalysts stability to coking is addition of molybdenum. It has been suggested that molybdenum-containing catalysts could possess

the highest coking stability for dry reforming of methane [28-30] and propane [31]. Hence, it might be expected that the addition of molybdenum oxide to perovskite-supported nickel catalyst should improve its coking resistance in steam reforming of oxygenates as well.

In this work, the effect of the preparation method and composition of catalysts based on perovskite-type ferrites on their structural, morphological, redox features and performance in ethanol steam reforming (ESR) has been studied.

2 Experimental

2.1 Catalysts preparation

Two series of catalysts based on praseodymium ferrite were prepared. The first series was $PrFe_{1-x}Ni(Co)_xO_3$ (x=0.3-0.4) perovskites prepared by modified Pechini route using metal (Me) nitrates, citric acid (CA), ethylene glycol (EG) and ethylenediamine (ED) as reagents [20-21]. The molar ratio of CA:EG:ED:Me was 3.75:11.25:3.75:1. CA and metal nitrates were dissolved in ethylene glycol at 80°C and in distilled water at room temperature, respectively. Prepared solutions were mixed together at room temperature under stirring followed by addition of ED. The mixed solution was heated at 70°C for 24 h allowing for the gel formation. The gel was calcined under air at 600°C, then obtained solids were ground and calcined at 900°C.

In the second series, 5%wt. Ni(Co)/$PrFeO_3$ catalysts were prepared by the incipient wetness impregnation of $PrFeO_3$ calcined at 700 and 900°C with nickel acetate or cobalt nitrate. Some oxidized/reduced samples of this series were modified with 5%wt. Mo. Ni-Mo were supported by successive or simultaneous impregnation with solutions of nickel nitrate and $(NH_4)_6Mo_7O_{24}$. All samples were dried and calcined at 500°C.

The chemical composition of catalysts is presented in Table 1.

2.2 Catalysts characterization

The catalysts were characterized by XRD, BET, TEM with EDX, H_2 temperature-programmed reduction. X-ray diffraction patterns were obtained with a D8 Advance diffractometer (Bruker) using CuKα radiation in 2θ scanning range 15–90° with step 0.05°. The structural refinement has been carried out using a PCW software (version 2.4). Qualitative phase analysis has been carried out by using PDF-2–ICDD files and ICSD/retrieve database. BET specific surface area (m^2/g) was determined from the data on Ar thermodesorption. The TEM micrographs were obtained with a JEM-2010 instrument (lattice resolution 1.4Å and acceleration voltage 200 kV). Local elemental analysis was performed with EDX method (a Phoenix Spectrometer).

The redox properties of catalysts were studied using temperature-programmed reduction (TPR) by H_2 using the flow of 10% H_2 in Ar, the feed rate 2.5 L/h, the temperature ramp from 25 to 900 °C at 10°/min. The experiments were carried out in kinetic installations equipped with GC Tcvet-500. In the case of repeated red-ox cycles, samples were reoxidized in the flow of O_2 for 1 h at 500 °C .

2.3 Catalytic performance tests

ESR was carried out in U-shaped tubular quartz plug-flow reactor (4.5 mm i.d.) at atmospheric pressure. Usually 0.18 g of pelletized catalyst (fraction 0.5-0.25 mm) diluted in a 1:10 weight ratio with quartz

Table 1: Methods of preparation, phase composition and BET area of the catalysts.

Catalyst	Preparation method	Calcination temperature, °C	Phase composition	S_{BET}, m^2/g
$PrFe_{0.7}Ni_{0.3}O_3$	Pechini	900	perovskite	7
$PrFe_{0.6}Ni_{0.4}O_3$	Pechini	900	Perovskite, NiO	10
$PrFe_{0.7}Co_{0.3}O_3$	Pechini	900	perovskite	3
$PrFe_{0.6}Co_{0.4}O_3$	Pechini	900	perovskite	3
$PrFeO_3$(700)	Pechini	700	perovskite	7
$PrFeO_3$(900)	Pechini	900	perovskite	4
5%Ni/$PrFeO_3$(900)	impregnation	900	perovskite, NiO	4
5%Ni/$PrFeO_3$(700)	impregnation	700	perovskite, NiO	7
5%Co/$PrFeO_3$(700)	impregnation	700	Perovskite, Co_3O_4	7
5%Ni+5%Mo/$PrFeO_3$(700)	simultaneous impregnation	700	perovskite, NiO, Mo&Ni-Mo oxides	6
5%Mo/5%Ni/$PrFeO_3$(700)	successive impregnation	700	Perovskite, NiO, Mo&Ni-Mo oxides	6
5%Mo/5%Ni_r/$PrFeO_3$(700)	Mo impregnation of reduced sample	700	Perovskite, NiO, Mo&Ni-Mo oxides	6

sand was taken. Reaction was performed at 500-800°C and 50000 h^{-1} GHSV (0.07 s contact time) using feed 10% C_2H_5OH+40% H_2O, N_2 balance. Before testing, the catalysts were pre-treated for 1 hour at 800 °C in the reaction feed or in the flow of 10 % H_2 in N_2. Three on-line gas chromatographs (GC) "LHM-8" equipped with thermal conductivity detectors and a flame ionization detector were used for the analysis of reactants and products. Hydrocarbons (CH_4, C_2H_6, C_2H_4, etc.) and oxygenates (EtOH, CH_3OH, acetone, diethyl ether, etc) were analyzed using a Porapak T column; N_2, O_2, CH_4 and CO were analyzed with a molecular sieve column, and H_2, N_2, CO, CO_2, CH_4 – with an active carbon "SYT" column. Ar and He were used as carrier gases. The coking of used catalysts was evaluated with temperature-programmed oxidation.

Ethanol conversion (X_{EtOH}), selectivity to carbon products (S_i) and hydrogen yield (Y_{H2}) were calculated according to the next equations:

$$x_{EtOH} = \frac{mol^{in}_{EtOH} - mol^{out}_{EtOH}}{mol^{in}_{EtOH}} \times 100\%,$$

$$S_i = \frac{\nu_i \cdot mol_i}{\sum_i^n \nu_i \cdot mol_i} \times 100\%,$$

$$Y_{H_2} = \frac{mol_{H_2}}{6 \cdot mol^{in}_{EtOH}} \times 100\%,$$

where n_i is the number of carbon atoms in "*i*" product.

3 Results and discussion

3.1 Structural and textural features

Characteristics of initial catalysts are presented in Table 1. The BET specific surface areas of perovskites are in the range of 3-10 m^2/g which are comparable with the usual values obtained for such systems [20-21, 24-26].

According to XRD data (Table 1, Fig.1-2), the main phase of all initial $PrFe_{1-x}Ni(Co)_xO_3$ (x=0-0.4) samples is orthorhombic perovskite with the lattice parameters being close to known values [32]. For the first series of samples, the presence of impurity phases is determined by the nature and content of doping cation: admixture of NiO phase appears at the highest nickel content (0.4), whereas all samples with cobalt remain the single-phase systems. As an example, the homogeneous distribution of elements is demonstrated using TEM with EDX data for $PrFe_{0.7}Ni_{0.3}O_3$ sample (Figure 3).

After reduction at 600°C in H_2, XRD patterns of perovskites are unchanged showing the retention of their structure (Figure 2). Reduction of samples at 800°C leads to the shift of perovskites reflections towards low angles and appearance of new reflections assigned to praseodymium oxide and Co(Ni)-Fe alloy (Figure 2). This shows a partial decomposition of perovskites: under reduction conditions Ni(Co) and a part of Fe are removed from the lattice, thus forming nanosized particles of Ni(Co)-Fe alloy stabilized on the surface of remaining perovskite.

For the second series of samples, the XRD patterns of starting catalysts show that they are comprised of Ni(Co) oxides and orthorhombic $PrFeO_3$. The broad reflections of Ni(Co) oxides indicate their high dispersion in catalysts based on $PrFeO_3$ calcined at 700 °C (Figure 4). This is confirmed by TEM with EDX data showing presence of small (<10 nm) NiO particles (Figure 5). EDX data suggest decoration of these particles by $PrFeO_x$ species (Figure 5). In the case of 5%Ni/$PrFeO_3$(900), the micrograph clearly

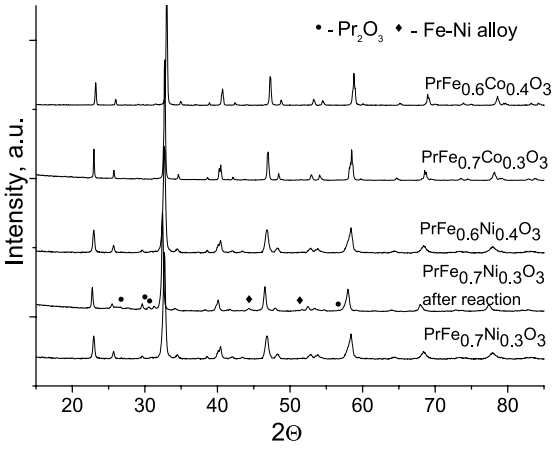

Figure 1: XRD-patterns of initial perovskites calcined at 900 °C and $PrFe_{0.7}Ni_{0.3}O_3$ used in ESR.

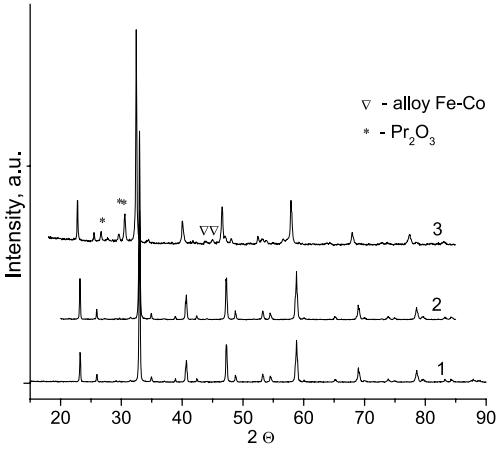

Figure 2: XRD patterns of initial $PrFeO_3$ calcined at 700 °C and supported 5%Co(Ni)/ $PrFeO_3$.

shows NiO particles of larger sizes. For Ni-containing catalysts doped with Mo, there are no reflections of Mo or mixed NiMo oxides in XRD patterns, while the data of TEM (Figure 6) show the presence of mixed Ni-Mo-oxides along with molybdenum oxide and NiO.

3.2 H_2-TPR

The typical H_2-TPR profiles for perovskites of the first series are presented in Figure 7. For $PrFe_{0.7}Ni(Co)_{0.3}O_3$, three main peaks are observed in the patterns: the intense low-temperature peak with the maximum at 354-381°C, the low intensity peak at 386-445°C and unresolved intense high-temperature peak above 600°C. The first low-temperature peak is assigned to reduction of $Ni(Co)^{3+}$ to $Ni(Co)^{2+}$, and the second one corresponds to reduction of Fe^{4+} cations to Fe^{3+} state within the perovskite lattice that is in agreement with known results [33] and our XRD data showing retention of perovskite structure after reduction at 600°C (Figure 4). The high-temperature peak is assigned to the partial destruction of perovskite structure with formation of Ni(Co)-Fe alloy and corresponding oxides. For $PrFe_{0.7}Co_{0.3}O_3$, the shift of the peaks to higher temperatures evidences more difficult reduction of Co-containing perovskites.

The H_2-TPR patterns for $PrFeO_3$ and supported 5%Ni(Co)/$PrFeO_3$ catalysts are presented in Figure 8. The spectrum of $PrFeO_3$ shows three main peaks: two low-intensity peaks at 413 and 477°C corresponding to the step-wise reduction of Fe^{4+} to Fe^{3+} and Fe^{2+} and partially resolved intense peak at 880°C due to further perovskite reduction [33]. The spectrum of 5%Co/$PrFeO_3$(700) shows two peaks at 335 and 386°C corresponded to reduction of Co_3O_4 [11] with a shoulder at 345°C indicating reduction of Fe^{4+} to Fe^{3+} in the perovskite support. For 5%Ni/$PrFeO_3$ catalysts, the spectrum profile strongly depends on the calcination temperature of $PrFeO_3$ support. Thus, in the spectrum of 5%Ni/$PrFeO_3$(900) with a low surface area, the intensive peak at 345 and a shoulder at 463°C are observed while a broad peak with maxima at 360 and 500 °C are present in the spectrum of 5%Ni/$PrFeO_3$(700) sample with a higher surface area. According to known data [12], the peaks below 400°C are related to reduction of NiO and peaks at 460-500° are ascribed to reduction of Fe^{4+} to Fe^{3+} in $PrFeO_3$ support [33]. The intense sharp peak at 345 °C shows a high uniformity of NiO crystallite size in the case of 5%Ni/$PrFeO_3$(900) sample. For 5%Ni/$PrFeO_3$(700) sample, a broad TPR peak suggests a wide size distribution of NiO particles and/or their stronger interaction with support that agrees with TEM/EDX data showing presence of oxidic nanoparticles containing

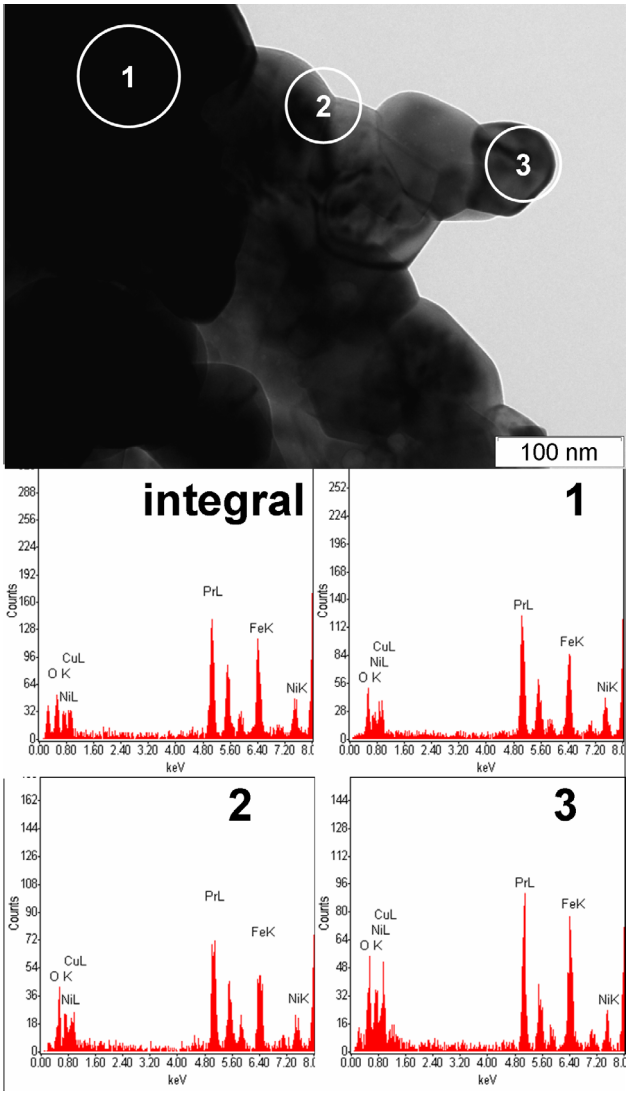

Figure 3: TEM micrographs and EDX of $PrFe_{0.7}Ni_{0.3}O_3$ calcined at 900°C.

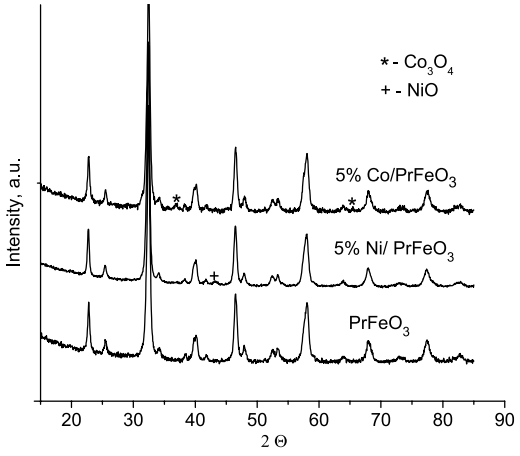

Figure 4: XRD-patterns of $PrFe_{0.6}Co_{0.4}O_3$: initial (1), reduced at 600 (2) and 800 °C (3).

simultaneously Ni, Pr and Fe cations (Fig.5). For all catalysts, the unresolved high temperature peak is due to further reduction of $PrFeO_3$.

The TPR spectra for 5%Mo+5%Ni/$PrFeO_3$(700) catalysts presented in Figure 9 show more symmetric profiles shifted to higher temperatures as compared with undoped 5%Ni/$PrFeO_3$(700) sample. Mo addition leads to disappearance of low-temperature hydrogen consumption. This could be due to formation of mixed Ni-Mo oxides as evidenced by TEM data (Figure 6). Besides, the reduction of catalysts depends on the method of Mo addition. Thus, in the case of the successive loading of Ni and Mo, the low-temperature peak corresponding to reduction of mixed oxide is shifted to higher temperatures by ~ 20° that could be due to blocking of NiO surface by molybdenum oxide.

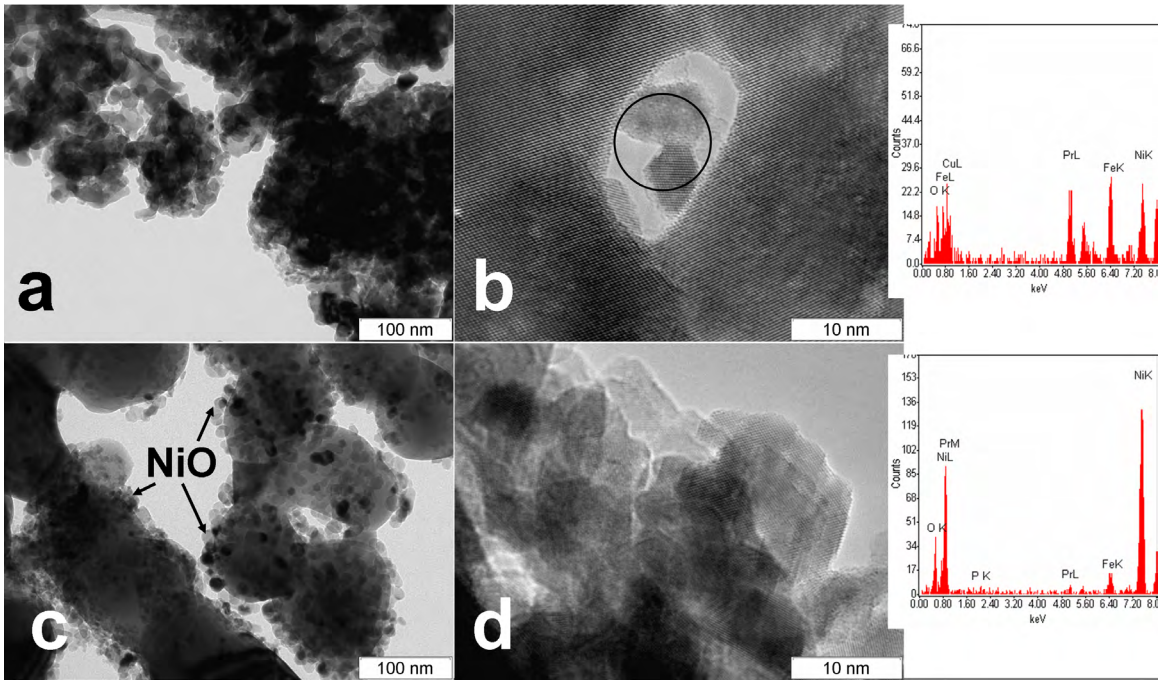

Figure 5: TEM micrographs of the initial catalysts with respective EDX spectra: a, b - 5%Ni/$PrFeO_3$(700) and c, d -5%Ni/$PrFeO_3$(900).

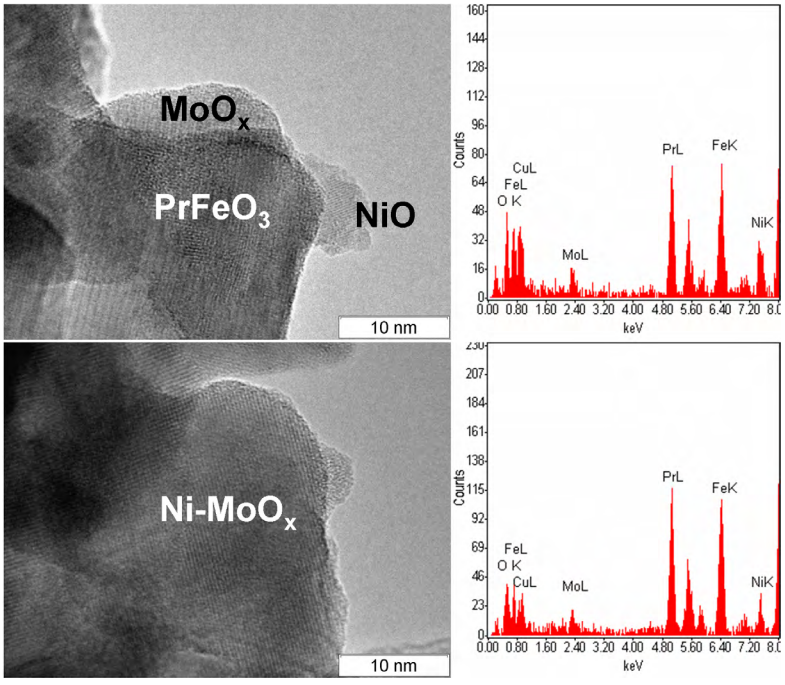

Figure 6: TEM micrographs and EDX of the initial 5%Mo/5%Ni/$PrFeO_3$ prepared by successive impregnation.

3.3 Steam reforming of ethanol

Temperature dependences of ethanol conversion, hydrogen yield and products selectivity for some catalysts of both series are presented in Figs. 10. In general, ethanol conversion is lower for the first series catalysts formed from perovskites precursors (Fig.10). Thus, over supported 5%Ni(Co)/$PrFeO_3$ catalysts of second series, ethanol conversion close to 100% is reached at 500-650°C while for catalysts of the first series it is reached above 700°C. In the first series of samples, the catalyst derived from $PrFe_{0.7}Ni_{0.3}O_3$ provides a higher ethanol conversion as compared with Co-containing ones.

Among the perovskite-supported catalysts, the ethanol conversion increases in the row: 5%Ni/$PrFeO_3$(700)<5%Co/$PrFeO_3$(700)<5%Ni/$PrFeO_3$(900). A high ethanol conversion for the sample 5%Ni/$PrFeO_3$(900) at temperature below 600°C could be due to easy reduction of NiO according to H_2-TPR data (Figure 8) that provides the effective activation of ethanol on metal particles. A lower ethanol conversion for 5%Ni(Co)/$PrFeO_3$(700) catalysts could be due to a strong interaction of supported active components with high surface area $PrFeO_3$(700) support leading to pronounced decoration of metal nanoparticles by oxidic PrFeOx fragments thus decreasing accessible metal surface area. In contrast to perovskite-derived catalysts, 5%Co/$PrFeO_3$(700) is more active as compared with 5%Ni/$PrFeO_3$(700).

The same trends as for ethanol conversion are observed for hydrogen yield, CO and CO_2 selectivity. Thus, the hydrogen yield of 90-95% is reached for 5%Ni/$PrFeO_3$(900) and 5%Co/$PrFeO_3$(700) at 600-650°, while the yield of 90% is only observed at 700° for $PrFe_{0.7}Ni_{0.3}O_3$ and at 800° for $PrFe_{0.6}Co_{0.4}O_3$ catalysts.

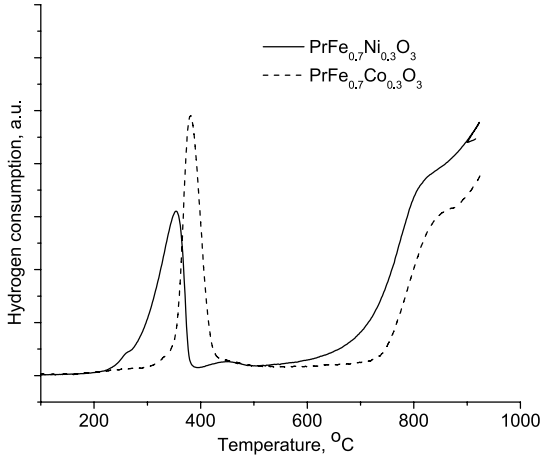

Figure 7: H_2-TPR spectra of $PrFe_{0.7}Co(Ni)_{0.3}O_3$.

The low C_2H_4 selectivity (<10%) and the presence of acetaldehyde (selectivity 15-60%) observed for catalysts of both series show that the main route of ethanol steam reforming corresponds to its dehydrogenation, though the presence of small C_2H_4 amount evidences some contribution of ethanol dehydration depending on the catalyst type. Thus, for 5%Ni/$PrFeO_3$(900) of a rather low Ni dispersion, C_2H_4 is not detected in all temperature range indicating only dehydrogenation route of ESR. In the case of 5%Ni(Co)/$PrFeO_3$(700) catalysts, a higher Ni/Co dispersion and decoration by support oxidic species leads to appearance of C_2H_4 showing some share of ethanol dehydration route. For catalysts derived from $PrFe_{1-x}Co_xO_3$, the highest C_2H_4 selectivity ~10% evidences a higher share of dehydration.

The effect of Mo doping and the method of its addition on ESR activity of 5%Ni/$PrFeO_3$(700) catalyst is illustrated in Figure 11. The ethanol conversion is only slightly influenced by Mo addition at temperatures above 650°C, while at 600°C some increase of ethanol conversion is observed for samples prepared by co-impregnation (5%Ni+5%Mo/$PrFeO_3$(700)) and impregnation of reduced catalyst (5%Mo/5%Ni_r/$PrFeO_3$(700)). At temperatures below 700°C, the conversion over 5%Mo/5%Ni/$PrFeO_3$(700) catalyst prepared by successive impregnation is the lowest among all catalysts that could be caused by blocking of Ni surface atoms with Mo. The lowest hydrogen yield for this sample is probably due to Ni blocking as well. At temperatures below 700°C, the highest hydrogen selectivity is observed for undoped 5%Ni/$PrFeO_3$(700) catalyst.

The values of C_2H_4 and acetaldehyde selectivities show that for Mo-doped catalysts, the main route of ESR is also dehydrogenation. At 550°C and the same ethanol conversion (Table 2), C_2H_4 selectivity is close for all catalysts while acetaldehyde selectivity is higher for Mo-doped samples. This could be due to blocking of active metal nickel by molybdenum that hinders acetaldehyde decomposition and formation of syngas. In addition, coordinatively unsaturated low-valence Mo cations/Mo-C

Table 2: Products selectivity and ethanol conversion at 550°C over catalysts 5%wt.Ni/$PrFeO_3$ and ones modified by Mo.

Catalyst	$X_{ethanol}$, %	Selectivity, %	
		C_2H_4	CH_3CHO
5%Ni/$PrFeO_3$(700)	48	5.5	10
5%Ni+5%Mo/$PrFeO_3$ Co-impregnation	48	6.5	22
5%Mo/5%Ni_r/$PrFeO_3$ Successive impregnation	48	5.7	25

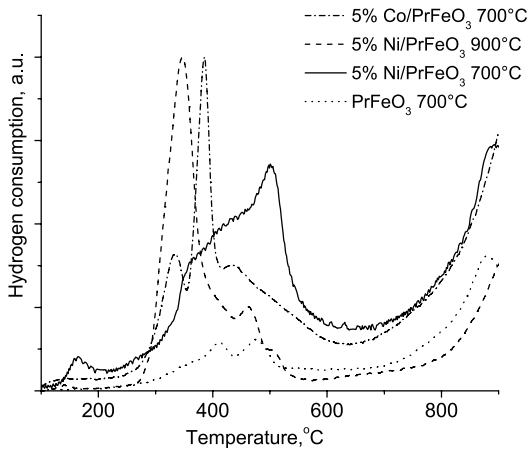

Figure 8: H_2-TPR spectra of initial $PrFeO_3$ and supported 5%Ni(Co)/ $PrFeO_3$.

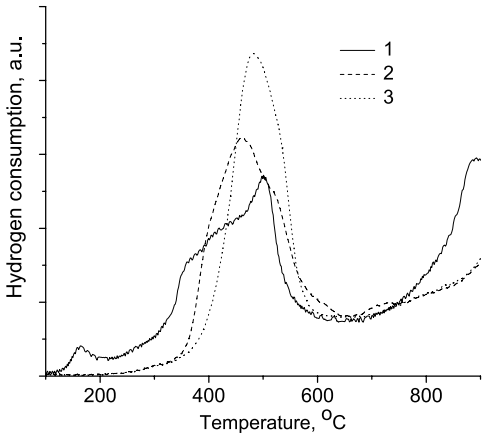

Figure 9: H_2-TPR spectra of 5% Ni/$PrFeO_3$ (700) (1) and 5% Mo + 5% Ni/$PrFeO_3$(700) prepared by: co-impregnation (2), successive impregnation of initial $PrFeO_3$(3).

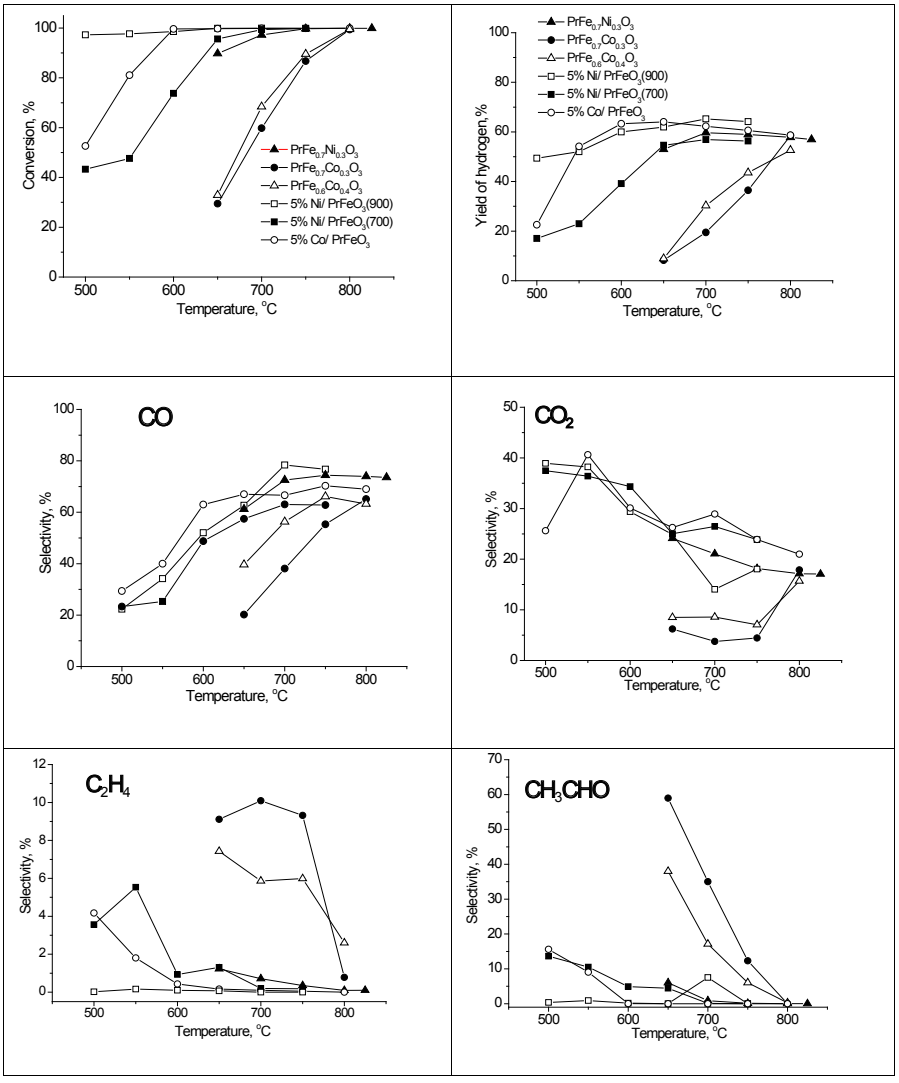

Figure 10: Ethanol conversion, hydrogen yield and products selectivity over perovskite-precursors and perovskite-supported catalysts.

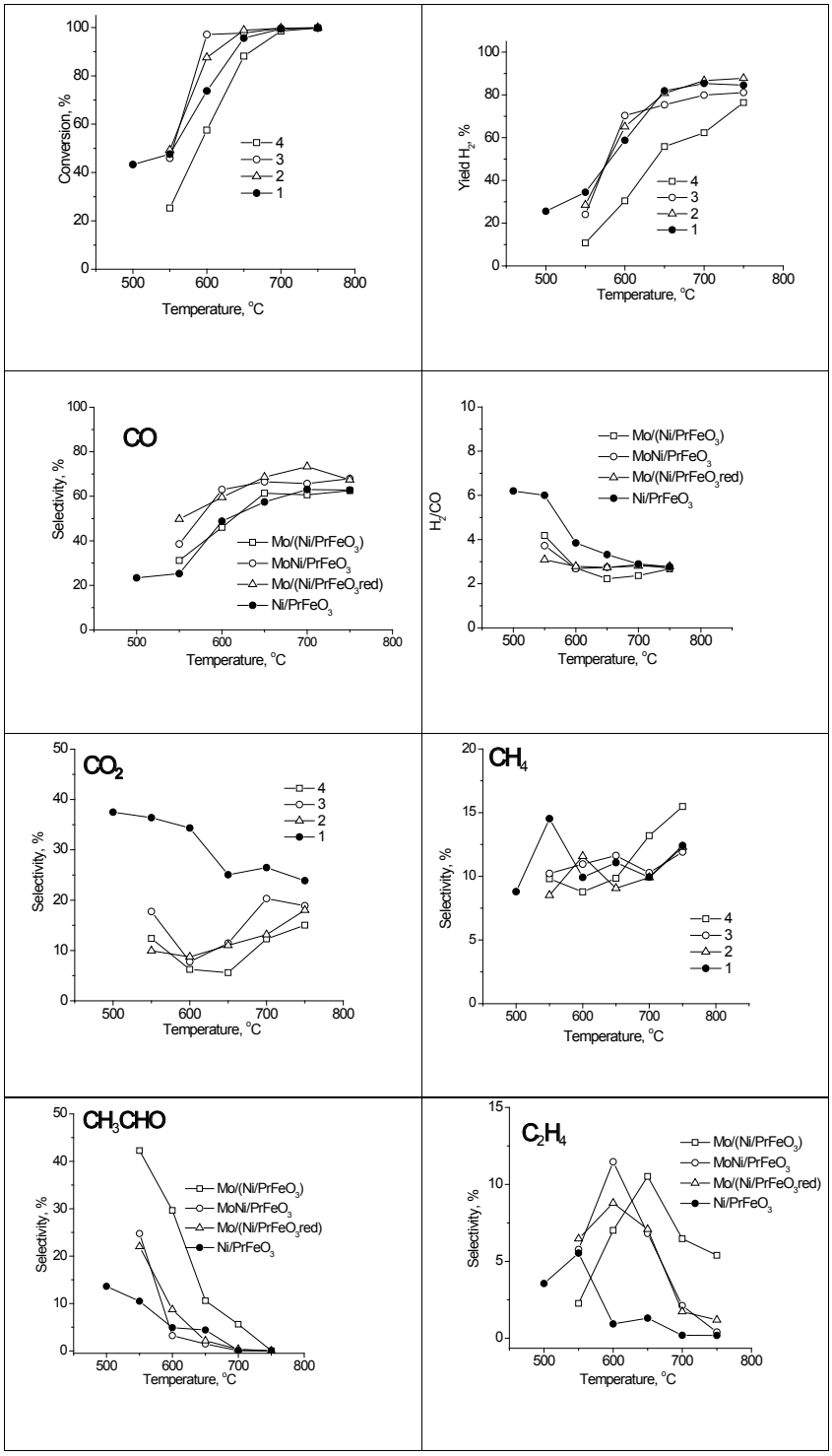

Figure 11: Ethanol conversion, hydrogen yield and products selectivity over supported 5%Ni/$PrFeO_3$ (1) and 5% Mo + 5% Ni/$PrFeO_3$ prepared by: impregnation of reduced 5% Ni/$PrFeO_3$ (2), co-impregnation (3) and successive impregnation of initial $PrFeO_3$(4).

fragments fixed at the perovskite particles surface could be involved in ethanol dehydrogenation as well.

The results of catalysts stability tests are presented in Figs. 12-13. Testing of catalysts in the diluted reaction mixture (10% C_2H_5OH+40% H_2O) at 650° reveals that the catalyst derived from $PrFe_{0.7}Ni_{0.3}O_3$ is more active and stable as compared with the sample based on $PrFe_{0.7}Co_{0.3}O_3$ (Figure 12). Note that strong coking of the latter is already observed after 2 hours testing. 5%Ni/$PrFeO_3$(700) and 5%Ni/$PrFeO_3$(900) catalysts with a high initial activity

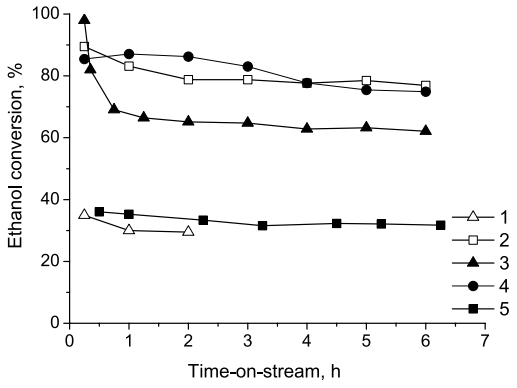

Figure 12: Time-on-stream testing of $PrFe_{0.7}Co_{0.3}O_3$(1), $PrFe_{0.7}Ni_{0.3}O_3$(2), 5%Ni/$PrFeO_3$(900) (3), 5%Ni/$PrFeO_3$(700) (4) and 5%Mo/5%Ni/$PrFeO_3$(700) (5) prepared by successive impregnation. The feed 10% C_2H_5OH+40% H_2O, N_2 balance, 650°C, contact time 0.07 s.

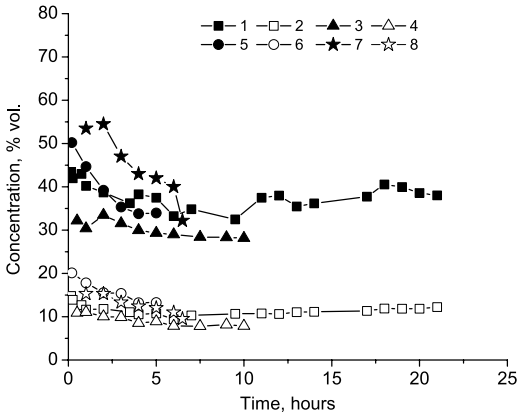

Figure 13: Concentration of H_2 (solid symbols) and CO (open symbols) during time-on-stream testing of $PrFe_{0.7}Ni_{0.3}O_3$ (1, 2), 5%Mo+5%Ni/$PrFeO_3$(700) prepared by successive (3,4) and simultaneous impregnation (5, 6), 5%Ni/$PrFeO_3$(700) (7,8). The feed 30% C_2H_5OH+60% H_2O, N_2 balance, 670°C, time contact 0.1 sec.

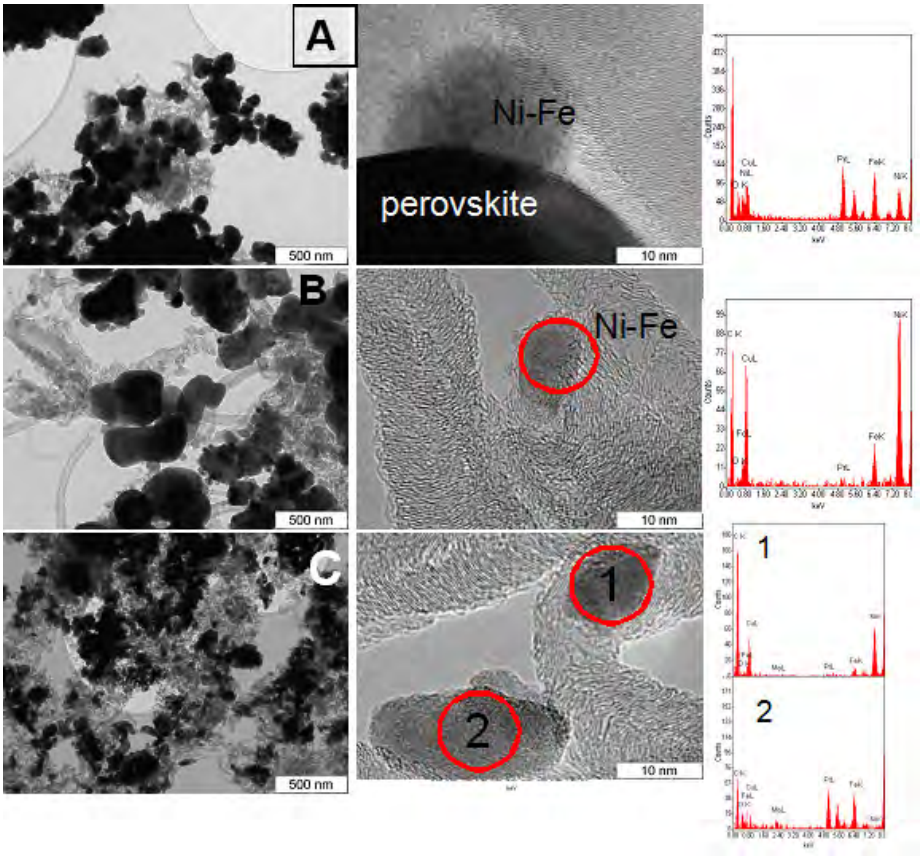

Figure 14: TEM with EDX of the catalysts after time-on-stream testing at different magnification. A - $PrFe_{0.7}Ni_{0.3}O_3$, 5%Ni/$PrFeO_3$(900) and 5%Mo/(5%Ni/$PrFeO_3$ (700) prepared by successive impregnation.

are more subjected to coking as compared to the doped 5%Mo/5%Ni/$PrFeO_3$(700) catalyst possessing a lower initial activity.

Results of both catalysts series testing in the real reaction mixture (30% C_2H_5OH+60% H_2O, N_2 balance) (Figure 12) in general coincide with those obtained in the diluted feed. However, coking of some supported catalysts occurs more rapidly due to higher ethanol concentration and a lower C_2H_5OH/H_2O ratio =2, which agrees with thermodynamic calculations showing that molar ratio

higher than 3 is required to avoid coke formation [34]. Thus, activity of the undoped supported catalyst 5%Ni/$PrFeO_3$(700) and 5%Mo+5%Ni/$PrFeO_3$(700) prepared by co-impregnation rapidly decreases due to severe coking, while $PrFe_{0.7}Ni_{0.3}O_3$ and 5%Mo/5%Ni/$PrFeO_3$(700) (successive impregnation) catalysts show satisfactory coking stability.

As a typical example, XRD pattern of used $PrFe_{0.7}Ni_{0.3}O_3$ catalyst is presented in Figure 1. According to XRD data, in the reaction media (similar to that in H_2 at 800°C) a partial decomposition of perovskite occurs with formation of Ni-Fe alloy, praseodymium oxide and remaining perovskite with modified lattice parameters. Hence, a high coking stability of the catalyst derived from $PrFe_{0.7}Ni_{0.3}O_3$ is due to its transformation into composite comprised of Ni-Fe alloy particles epitaxially bound with remaining $PrFeO_3$ perovskite particles. Such alloy particles of a high dispersion are less subjected to coking as TEM images demonstrate in Figure 14A. In the case of perovskite-supported catalysts, the bonding of Ni-Fe alloy particles with $PrFeO_3$ support is weaker, their dispersion is lower and these catalysts are strongly subjected to coking with formation of filamentous deposits that leads to detachment of Ni-Fe alloy particles and their encapsulation (Figure 14 B, C). A higher coking stability of 5%Mo/5%Ni/$PrFeO_3$(700) catalyst prepared by successive impregnation could be due to formation of molybdenum carbide on the catalyst surface under reaction conditions [29].

4 Conclusions

For two series of catalysts based on praseodymium ferrite, structural and redox properties as well as performance in ethanol steam reforming have been studied. The first series is based on $PrFe_{1-x}Ni(Co)_xO_3$ (x=0.3-0.4) perovskites prepared by modified Pechini route, and the second one includes 5%wt.Ni(Co)/$PrFeO_3$ catalysts of different dispersion (some samples being modified by 5%wt. Mo) prepared by impregnation of $PrFeO_3$. At temperatures above 700°C, for all catalysts, the main products were hydrogen and CO. At temperatures below 700°C, the initial ethanol conversion and hydrogen yield were higher for supported catalysts as compared with ones derived from Ni(Co)-containing perovskites. While Ni-based catalysts derived from perovskite were more active as compared with Co-based samples, perovskite supported 5%Co/$PrFeO_3$(700) has shown a higher initial activity as compared with 5%Ni/$PrFeO_3$(700). The long-term tests in the realistic feed and TEM study of spent catalysts revealed that perovskite-derived catalysts have a higher coking stability than perovskite-supported ones due to formation of highly dispersed Ni-Fe alloy particles strongly interacting with parent perovskite matrix. The method of Mo supporting only slightly influencing the initial activity of Ni/$PrFeO_3$ catalysts noticeably affects their coking stability: 5%Mo/5%Ni/$PrFeO_3$(700) catalyst prepared by successive impregnation shows the highest stability among perovskite-supported catalysts.

Acknowledgements: This work is supported by Integration Project 8 of SB RAS-NAN Belarus, Russian Fund of Basic Research Project RFBR-CNRS 12-03-93115; Federal Program "Scientific and Educational Cadres of Russia".

Received: October 16, 2013; Accepted: December 09, 2013.

References

[1] Kirtay E., Energy Conversion and Management, 2011, 52, Recent advances in production of hydrogen from biomass, 1778-1789.
[2] Tanksale A., Beltramini J. N., Lu G. M., A review of catalytic hydrogen production processes from biomass, Renew. Sustainable Energy Rev., 2010, 14, 166-182.
[3] Chattanathan S. A., Adhikari S., Abdoulmoumine N., A review on current status of hydrogen production from bio-oil, Renew. Sustainable Energy Rev., 2012, 16, 2366-2372.
[4] Haryanto A., Fernando S., Murali N., and Adhikari S., Current status of hydrogen production techniques by steam reforming of ethanol: A review, Energy & Fuels, 2005, 19, 2098-2106.
[5] Vaidya P.D., Rodrigues A.E., Insight into steam reforming of ethanol to produce hydrogen for fuel cells, Chem. Eng. J., 2006, 117, 39-49.
[6] Yung M. M., Jablonski W. S., and Magrini-Bair K. A., Review of Catalytic Conditioning of Biomass-Derived Syngas, Energy & Fuels, 2009, 23, 1874-1887.
[7] Slinn M., Kendall K., Mallon C., Andrews J., Steam reforming of biodiesel by-product to make renewable hydrogen, Bioresource Technology, 2008, 99, 5851-5858.
[8] Basagiannis A. C., Verykios X. E., Reforming reactions of acetic acid on nickel catalysts over a wide temperature range, Appl. Catal. A Gen., 2006, 308, 182-193.
[9] Hu X., G. L., Investigation of the steam reforming of a series of model compounds derived from bio-oil for hydrogen production, Appl. Catal. B Environ., 2009, 88, 376-385.
[10] Fatsikostas A. N., Verykios X. E., Reaction network of steam reforming of ethanol over Ni-based catalysts, J. Catal., 2004, 225, 439-452.
[11] Batista M. S., Santos R. K. S., Assaf E. M., Assaf J. M., Ticianelli E. A., High efficiency steam reforming of ethanol by cobalt-based catalysts. J. Power Sources, 2004, 134, 27-32.
[12] Biswas P., Kunzru D., Oxidative steam reforming of ethanol over Ni/CeO_2-ZrO_2 catalyst, Chem. Eng. J., 2008, 136, 41-49.
[13] Lima S. M., Silva A. M., Costa L.O.O., Graham U. M., Burtron G. J., Davis H., Mattos L. V., Noronha F. B., Study of catalyst deactivation and reaction mechanism of steam reforming,

partial oxidation, and oxidative steam reforming of ethanol over Co/CeO_2 catalyst. J. Catal., 2009, 268, 268-281.

[14] Costa L.O.O., Silva A. M., Noronha F. B., Mattos L.V., The study of the performance of Ni supported on gadolinium doped ceria SOFC anode on the steam reforming of ethanol, Int. J. Hydr. Energy, 2012, 37, 5930-5939.

[15] Liguras D. K., Kondarides D. I., Verykios X. E., Production of hydrogen for fuel cells by steam reforming of ethanol over supported noble metal catalysts, Appl. Catal. B, 43, 2003, 345-354.

[16] Rioche C., Kulkarni S., Meunier F. C., Breen J. P., Burch R., Steam reforming of model compounds and fast pyrolysis bio-oil on supported noble metal catalysts, Appl. Catal. B, 2005, 61, 130-139.

[17] Lima S.M., Silva A.M., Costa L.O.O., Graham U.M., Burtron G. J., Davis H., Mattos L.V., Noronha F.B., Ethanol decomposition and steam reforming of ethanol over $CeZrO_2$ and Pt/$CeZrO_2$ catalyst: Reaction mechanism and deactivation, Appl. Catal. A, 2009, 352, 95-113.

[18] Wang F., Cai W., Provendier H., Schuurman Y., Descorme C., Mirodatos C., Shen W., Hydrogen production from ethanol steam reforming over Ir/CeO_2 catalysts: Enhanced stability by PrOx promotion, 2011, 36, 13566-13574.

[19] Ramos A.C., Montini T., Lorenzut B., Troiani H., Gennari F.C., Graziani M., Fornasiero P., Hydrogen production from ethanol steam reforming on M/CeO_2/YSZ (M = Ru, Pd, Ag) nanocomposites, Cat. Today, 2012, 180, 96-104.

[20] Kapokova L., Pavlova S., Bunina R., Alikina G., Krieger T., Ishchenko A., Rogov V.and Sadykov V., Dry reforming of methane over $LnFe_{0.7}Ni_{0.3}O_{3-\delta}$ perovskites: Influence of Ln nature, Catal. Today, 2011, 164, 227-233.

[21] Pavlova S., Kapokova L., Bunina R., Alikina G., Sazonova N., Krieger T., Ishchenko A., Rogov V., Gulyaev R., Sadykov V. and Mirodatos C., Syngas production by CO_2 reforming of methane using LnFeNi(Ru)O_3 perovskites as precursors of robust catalysts Catal. Sci. Technol., 2012, 2, 2099-2108.

[22] Chen H., Yu H., Peng F., Yang G., Wang H., Yang J., Tang Y., Autothermal reforming of ethanol for hydrogen production over perovskite $LaNiO_3$, Chem. Eng. J., 2010, 160, 333-339.

[23] Lima S.M., Silva A.M., Costa L.O.O., Assaf J.M., Jacobs G., Davis B.H., Mattos L.V., Noronha F.B., Evaluation of the performance of Ni/La_2O_3 catalyst prepared from $LaNiO_3$ perovskite-type oxides for the production of hydrogen through steam reforming and oxidative steam reforming of ethanol, Appl. Catal. A, 2010, 377, 181-190.

[24] Chen S.Q., Wang H., Liu Y., Perovskite La–St–Fe–O (St=Ca, Sr) supported nickel catalysts for steam reforming of ethanol: The effect of the A site substitution, Int. J. Hydr. Energy, 2009, 34, 7995-8005.

[25] Chen S.Q., Li Y.D., Liu Y., Bai X., Regenerable and durable catalyst for hydrogen production from ethanol steam reforming, Int. J. Hydr. Energy, 2011, 36, 5849-5856.

[26] Lima S. M., Silva A. M., Costa L.O.O., Assaf J.M., Mattos L.V., Sarkari R., Venugopale A., Noronha F.B., Hydrogen production through oxidative steam reforming of ethanol over Ni-based catalysts derived from $La_{1-x}Ce_xNiO_3$ perovskite-type oxides, Appl. Catal. B: Env., 2012, 121– 122, 1-9.

[27] Urasaki K., Tokunaga K., Sekine Y., Matsukata M., Kikuchi E., Production of hydrogen by steam reforming of ethanol over cobalt and nickel catalysts supported on perovskite-type oxides, Cat. Comm., 2008, 9, 600-604.

[28] York A. P. E., Suhartanto T.and Green M.L.H., Influence of molybdenum and tungsten dopants on nickel catalysts for the dry reforming of methane with carbon dioxide to synthesis gas, in: Parmaliana A. et al. (Eds), Studies in Surface Science and Catalysis, Elsevier Science, 1998, Vol. 119, p.777.

[29] Zhang A., Zhu A., Chen B., Zhang S., Au C., Shi C., In-situ synthesis of nickel modified molybdenum carbide catalyst for dry reforming of methane, Cat. Comm., 2011, 12, 803–807.

[30] Cheng J., Huang W., Effect of cobalt (nickel) content on the catalytic performance of molybdenum carbides in dry-methane reforming, Fuel Proc. Tech., 2010, 91, 185–193.

[31] Siahvashi A., Chesterfield D., Adesina A.A., Propane CO_2 (dry) reforming over bimetallic Mo–Ni/Al_2O_3 catalyst, Chem. Eng. Sci., 2013, 93, 313–325.

[32] R. Kumar, R. J. Choudhary, M. Ikram, D. K. Shukla and S. Mollah, P. Thakur and K. H. Chae, B. Angadi and W. K. Choi, Structural, electrical, magnetic, and electronic structure studies of $PrFe_{1-x}Ni_xO_3$ (x<0.5), J. Appl. Phys., 2007, 102, 073707-1-9.

[33] Provendier H., Petit C., Estournes C., Libsa S., and Kiennemann A., Stabilisation of active nickel catalysts in partial oxidation of methane to synthesis gas by iron addition, Appl. Catal. A, 1999, 180, 163-173.

[34] Mas V., Kipreos R., Amadeo N., Laborde M., Thermodynamic analysis of ethanol/water system with the stoichiometric method, Int. J. Hydr. Energy, 2006, 31, 21-28.